International Research Journal of Engineering and Technology (IRJET) e-ISSN: 2395-0056
Volume: 10 Issue: 05 | May 2023 www.irjet.net p-ISSN: 2395-0072

THERMODYNAMIC ANALYSIS OF SOLAR POWERED COMBINED SUPERCRITICAL CARBON DIOXIDE CYCLE AND ORGANIC RANKINE CYCLE.

Miss. Reshma R Bangar[1], Prof. Ajay Kashikar [2], Prof. Rajesh Kumar [3]

[1]Student, Department of Mechanical Engineering, Alamuri Ratnamala institute of engineering and technology, Shahpur, Thane Maharashtra, India
[2] Assistant Professor, Department of Mechanical Engineering, Lokmanya Tilak College of Engineering, Koparkhairne, Navi-Mumbai, Maharashtra, India
[3] Assistant Professor, Department of Mechanical Engineering, Alamuri Ratnamala institute of engineering and technology, Shahpur, Thane Maharashtra, India

---

Abstract - Thermodynamic analysis of the combined partial heating supercritical CO2 (PSCO2) cycle and ORC is presented in this study. In engineering equation solver software, a computer program was created for parametric analysis of the model. Basic PSCO2 cycle was then compared with existing previous studies that were conducted without partial heating. It was concluded that the PSCO2 system was 1 to 3% thermally more efficient than the non-partial heating cycle. Furthermore, it was found that ORC's use in existing PSCO2 cycle improved thermal efficiency by 4.47% of the basic PSCO2 cycle. The effects of the parabolic trough collectors (PTSCs) on the combined cycle performance were further examined. Without taking into account the performance of the PTSCs, the highest exergy and thermal efficiency of the combined cycle using R1233zd(E) was achieved by 83.26 and 48.61%, respectively at 950 W/m2 of solar irradiation while taking into account the performance of PTSCs, the combined cycle achieved exergy efficiency by 42.31% because PTSCs alone accounted for 62.93% of the total exergy destruction. One of the other conclusions obtained from the results was that the highest solar incidence angle was responsible for poor system performance.

Key Words: **Thermodynamic analysis; parabolic trough solar collector; partial heating supercritical CO2 cycle; ORC**

1. INTRODUCTION

Nowadays, there is a high demand for energy due to the increasing population and the development of industries (Yagli 2020). This leads to an increase in the generation of more power. But conventional energy resources are steadily declining. That is why dependence on renewable energy resources is simultaneously increasing. The renewable energy resources currently being used for the generation of electricity is geothermal energy, wind energy, solar energy, etc. Compared to other renewable energy sources, solar energy is low-cost, noise-free, and abundantly freely available in nature (Tiwari, Sherwani, and Kumar 2018). Previous studies have shown that, among other renewable energy resources, solar energy for cooling, heating, and power generation is the most appropriate energy resource (Abdelghani-Idrissi et al. 2018). Solar collectors are used for the use of solar energy. The heat transfer fluid takes heat from solar thermal energy inside the collectors. In addition, this heat transfer fluid is used for driving different types of thermodynamic cycles (Desai and Bandyopadhyay 2016). Parabolic trough solar collector (PTSC) is used for collecting solar heat to heat high or medium temperature fluids. Selection of PTSCs is optimum due to acceptable cost and higher efficiency among the other solar collectors (Cabrera et al. 2013). In addition, there are numerous studies based on the performance of the PTSC. It is used for driving the various power generation cycles such as the steam Rankine cycle (Al-Sulaiman 2013), the Kalina cycle (Ashouri et al. 2015), the organic Rankine cycle (Desai and Bandyopadhyay 2016), the cogeneration systems and the hybrid conventional-solar power cycle. Some solar-driven systems could not have become so popular due to non-clean energy systems (Bellos and Tzivanidis 2016). Supercritical CO2 (SCO2) is the state of CO2 above its critical point (304.13 K, 7.38 MPa). The SCO2 cycle uses SCO2 as the working fluid. SCO2 cycle is one cycle that can be used to harvest heat from different heat sources such as geothermal energy, natural gas, coal power, solar thermal energy, exhaust gas waste heat (Ahn et al. 2015). Some configurations of the SCO2 cycles for the use of heat from different thermal energy resources are simple supercritical cycle, single-heated cascade cycle, recompression, pre-compression, partial heating, dual cascade cycle, single-heated cascade cycle with intercooler, dual-heated cascade cycle with intercooler, dual-heated and triple-heat flow split cycles, dual-expansion cycles with intercooler. Among these SCO2 cycles, detailed analysis of certain cycles such as (simple

recuperated cycle (Singh and Mishra 2018a), recompression cycle (Singh and Mishra 2018b) was carried out using solar energy as a heat source considering ORC as the bottom cycle. In addition, a detailed analysis is needed to investigate the performance of the partial heating cycle (Campanari and Macchi 1998) because it has a small number of components, simple layout and simple operation due to single turbine and single compressor. The partial heating cycle was considered during the recompression cycle due to the same number of heat exchangers and produces more power compared to the recompression cycle. But it has more flow points and heaters than the recompression cycle, so further investigation can be carried out to investigate the effects of these additional heaters. The heating cycle is therefore suitable for the future MW heat source (Kim et al. 2016).

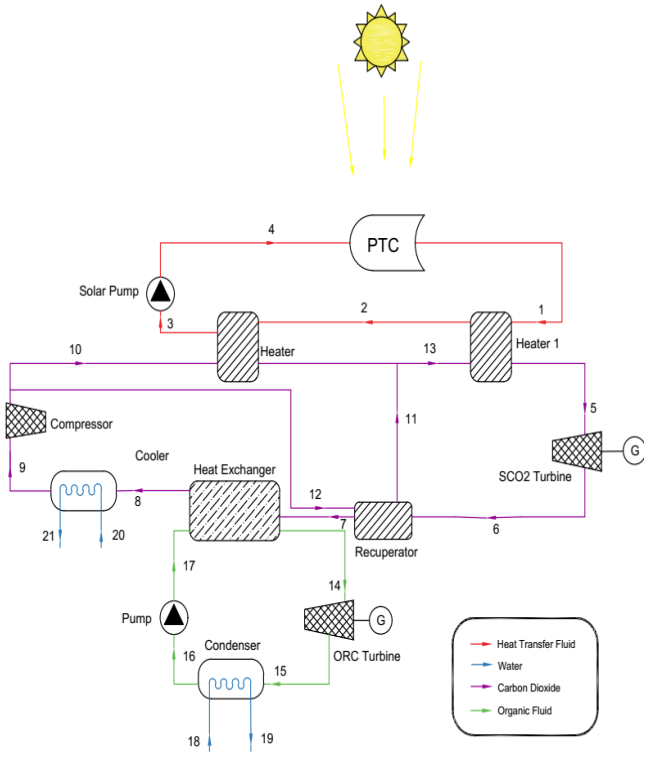

Figure 1 Schematic diagram of solar integrated combined (PSCO2–ORC) system

A detailed study was conducted on some SCO2 cycles, such as (Fan et al. 2020) proposed a combined sCO2 and trans-critical carbon dioxide (tCO2) cycle as a bottoming cycle. Further multiobjective optimization was performed on the part load condition. They concluded that when the temperature variation of the heat sink was 5–25°C, the combined sCO2–tCO2 cycle could operate within 10–100% of the normalized generator and the corresponding exergetic efficiency of the combined sCO2–tCO2 cycle ranged from 24.5 to 65.7% (Khatoon and Kim 2020) performed detailed analysis of the supercritical carbon dioxide recompression Brayton cycle and the tCO2 cycle as a bottoming cycle assisted with concentrated solar power (CSP) cycle. They found that the efficiency of the combined cycle was enhanced by the use of waste heat and reduced the flow of cooling water. The combined cycle efficiency increased first and then decreased with an increase in the maximum temperature of the cycle. A few studies were conducted on combined SCO2 cycles and ORC.ORC cooperated as a low temperature cycle to recover waste heat from those cycles. (Singh and Mishra 2018a) carried out an energy and energy analysis on the model of integrated solar PTSCs, combined with the simple recuperated SCO2 cycle and the ORC as a bottoming cycle. They concluded that the system's exergetic and energetic efficiency increased with solar irradiation. In addition, the fuel depletion ratio and the highest power output were found to be 0.2583 and 3740 kW, respectively, at 0.85 kW/m2 of solar irradiation. (Singh and Mishra 2018b) investigated the thermal performance of the solar operated combined recompression SCO2 and ORC as a bottoming cycle. They found that the combined system's thermal and energy efficiency increased with solar radiation and turbine inlet pressure. R123 and R290 showed the best and worst thermal performance of the system. In addition, they also concluded that the solar collector was responsible for the maximum exergy destruction of the system. (Besarati and Goswami 2014) examined the different configurations of the SCO2 cycles, such as simple recuperated, recompression and partial cooling of the SCO2 cycles. These cycles, combined with ORC as a bottoming cycle, have also been examined for the concentration of solar power applications. They concluded that the recompression cycle was more promising, especially for the use of solar power. Recompression cycles combined with ORC also achieved higher efficiency among other selected cycles. (Al-Sulaiman, Hamdullahpur, and Dincer 2012) conducted a study to investigate the performance of novel combined integrated PTSC systems with ORC for tri – generation applications, i.e. heating, cooling and power generation at the same time. Simultaneously, a fraction of ORC waste was used for cogeneration (cooling, heating) and the effect of deferent parameters on system performance and efficiency improved from 15 to 94% in solar mode. (Wang and Dai 2016) carried out an exergoeconomic and comparative analysis of the SCO2/tCO2 and SCO2/ORC configurations and found that the SCO2/tCO2 cycle performs better than the SCO2/tCO2 cycle at a lower compression ratio. In addition, it was found that the SCO2/tCO2 cycle has a slightly lower total unit cost value compared to the SCO2/ORC. Further, few researchers considered the integrated PTSC with ORC for various applications such as waste heat recovery and cogeneration process. (Nafey and Sharaf 2010) conducted a thermodynamic (exergetic and energetic) analysis of solar PTSC integrated ORC system for obtaining power to drive reverse osmosis (RO) desalination system. (Delgado-Torres, García-Rodríguez,

and Romero-Ternero 2007) conducted detailed energy analysis (thermal) of PTSC integrated ORC system coupled with RO unit for production of potable water. Numerous investigations were conducted in another study (Delgado-Torres and García-Rodríguez 2010a) on the solar integrated RO desalination system for brackish water and seawater. They also concluded that solar-powered RO production has reached its maximum value, i.e., a 2% blow using R245fa. They also conducted research to examine the effect of different working fluids such as butane, isobutene, R245ca, and R245fa on the aperture area of the PTSC system for water desalination and power generation (Delgado-Torres and García-Rodríguez 2010b). (Yagli et al. 2019) designed and optimized the solar power tower assisted steam cycle. Thermal efficiency and net power were found to be 45.814% and 47,046.60 kW, respectively, for the best performing conditions. In addition, overall exergy efficiency was found to be 47.19%. From the literature review, it was observed that no study was conducted on the basis of the thermodynamic analysis of the PTSC-driven combined partial heating SCO2 cycle and ORC (PSCO2–ORC). The study has novelty due to the application of the PTSC and ORC to the existing partial heating SCO2 cycle. Main objective of the study was to investigate the effects of PTSC and ORC on the PSCO2 cycle performance. Subsequently, results were compared with previous existing studies performed without partial heating. Thermal efficiency, exergy efficiency and exergy destruction rate were considered to be performance parameters for the proposed system. The effects on the system performance of solar irradiation, turbine inlet pressure, solar incidence angle and split ratio and recuperator efficiency were investigated. The performance of the proposed system was also analyzed with and without PTSCs.

2. DESCRIPTION

Solar PTSC integrated combined partial heating SCO_2 and ORC as a waste heat recovery cycle. In the considered model, the partial heating SCO_2 cycle is a topping cycle and for waste heat utilization ORC is considered as bottoming cycle which is directly coupled with SCO_2 cycles. The temperature entropy (T-s) diagram of the proposed model All states are corresponding to schematic diagram of current model. In the combined cycle ($PSCO_2$–ORC) expansion of high temperature and pressure SCO_2 occurs in SCO_2 turbine (state 5 to 6) up to lower pressure and temperature. Then it passes through recuperator (state 6 to 7), after recuperation process, this stream passes the heat exchanger (state 7 to state 8), where it transfers sufficient amount of thermal energy to drive ORC. Also, the stream passes through a cooler (state 8 to 9) to cool itself for getting required critical conditions of carbon dioxide. After the cooler, it passes through the compressor unit (state 9 to10) where again temperature and pressure increase. Further, a fraction of the mass of SCO_2 passes through the second heater (state 10 to 12) where stream extracts heat from heat transfer fluid (HTF) syltherm 800, which is circulating in PTSC fields. Apart from this, the remaining part of stream passes through recuperator (state 10 to 11) where stream preheats. At state 13, both streams mix each other than enters in high temperature first heater where SCO_2 extract heat from HTF, which is circulating in PTSC fields. At last, it again enters in turbine and completes the cycle.

3. WORKING FLUID SELECTION

The selection of proper working fluids for the system is challenging because it affects system performance, economic feasibility, efficiency, and operating conditions. It is better if the critical temperature of the working fluid is near the source or waste heat temperature (Abam et al. 2018). In the current study, 'Syltherm 800' was selected as an HTF in the absorber tube of the solar collector to absorb solar heat due to its maximum working temperature of 420°C (Singh and Mishra 2018a). Thermo physical properties of 'Syltherm 800' are shown in Table 2. The working fluids in the ORC system should have the optimum thermo physical and thermodynamic properties at optimum pressure and temperature and must also be nontoxic, ecofriendly, economical, and safe and use heat energy efficiently from the heat source (Kose, Koc, and Yagli 2020). In addition, the chemical composition of organic working fluids deteriorates above the maximum temperature of the fluid, which may cause system instability (Koc, Yagli, and Koc 2019). These six working fluids (R1224 yd(Z), R1234ze(Z), R1234yf, R1234ze(E), R1233zd(E) and R1243zf) were considered for analysis considering these criteria and for low temperature application. Thermo-physical properties of these working fluids are shown in Table 3.

Table 2. Thermophysical properties of Syltherm 800 at 650 K (Mwesigye, Bello-Ochende, and Meyer 2014). Thermo-

physical properties	Numeric data
Density (ρ)	577.70kg/m3
Viscosity ðμÞ	0.000284Pa-s
Thermal conductivity (k)	0.067833(W/m-K)
Specific heat capacity c_p	2.218 (kJ/kg -K)

Table 3. Organic working fluid's properties (Eyerer et al. 2019; Fukuda et al. 2013; Lai 2014. Singh and Mishra 2018a).

Fluids	Weights (kg/k-mole)	Critical temp.,(^0 C)	Critical pressure(MPa)	ODP	GWP
R1243zf	96.05	104.44	3.6306	0	.
R1234ze(E)	114.043	109.4	3.64	0	6
R1234yf	114.04	94.7	4.597	0	<1
R1234ze(Z)	114.04	150.1	3.53	0	<10
R1224 yd(Z)	148.5	155.5	3.33	0.00023	0.88
R1233zd(E)	130.5	165.5	3.57	0.00024	7

4.EFFECT ON SYSTEM PERFORMANCE OF INTENSITY OF SOLAR IRRADIATION

Variation of the solar radiation intensity has a significant impact on the thermodynamic performance of the proposed system. At the beginning of this section, the effect of solar irradiation on the stand alone PSCO2 cycle was examined. As solar irradiation increased from 0.5 to 0.95 kW/m2 exergy and thermal efficiency improved by 29.77 and 30.52%, respectively, , while the exergy destruction rate decreased by 50.40% it can be seen that the exergetic efficiency of the combined system (PSCO2–ORC) improves with solar radiation because solar radiation is effectively utilized by solar collectors (Singh and Mishra 2018a). It varies from 63.70% at 0.5 kW/m2 to 83.26% at 0.950 kW/m2 on the basis of R1233zd(E). The PSCO2 cycle plays a key role in improving the efficiency of the combined cycle. the addition of PTSC to the combined cycle of exergy efficiency of the whole plant (PTSC–PSCO2–ORC) is reduced due to more exergy destruction in solar collectors. The exergy efficiency of the whole plant increases from 18.63% at 0.5 kW/m2 to 42.31% at 0.95 kW/m2 continuously on the basis of R1233zd(E). According to Eq. (52), thermal efficiency of the combined cycle increases continuously with solar irradiation as can be seen in Figure 10. Based on R1233zd(E) as solar irradiation increases from 0.50 to 0.95 kW/m2 thermal efficiency is improved by nearly 28.90% while R1243zf shows worst performance. Exergy destruction rate of the combined cycle and whole plant show reveres trend with the solar irradiation. As solar irradiation increases from 0.5 to 0.95 kW/m2 the exergy destruction rate of the combined cycle and whole plant decreased by 47.36 and 27.50%, respectively, on the basis of R1233zd(E) which is the lowest of the selected working fluids, while R1243zf shows the highest exergy destruction rate. Comparison the total plant (PTSC–PSCO2–ORC) is comparatively higher exergy destruction rate than the combined system (PSCO2–ORC) due to more exergy input into the collector field at the same time less exergy conversion to working fluid (Singh and Mishra 2018a). It has also been calculated that PTSC has a large amount of exergy destruction varying from 8567.01 kW at 0.50 kW/m2 to 4745.39 kW at 0.95 kW/m2.

5. CALCULATION

EES is an abbreviation for Engineering Equation Solver. The simple function delivered by EES is the explanation of a set of algebraic equations. EES can also solve differential equations, equations with complex variables, perform optimization, offer non-linear and linear regression, generate publication-quality plots, abridge and analyses complex applications and deliver animations. EES tool has been used in different Mechanical Engineering courses such as heat transfer, gas dynamics, thermodynamics and Capstone. EES includes the material properties; therefore, the students enjoyed using EES in mechanical engineering courses and in particular thermo-fluid courses [18].

The available solar energy on the collector aperture is calculated as the product of the collector aperture (A_a) and of the direct beam solar irradiation (G_b), as it is presented below [19]:

$$Q_s = A_a \times G_b Q_s = A_a \times G_b \quad (1)$$

The tubular absorber absorbs a lower quantity of energy (Q_{abs}) due to optical losses, as equation 2 shows:

$$Q_{abs} = Q_s \times \eta_{opt} Q_{abs} = Q_s \times \eta_{opt} \quad (2)$$

The optical losses are expressed with the optical efficiency (η_{opt}). More specifically, the concentrator reflectance (ρ), the intercept factor (γ), the cover transmittance (τ), the absorber absorbance (α), as well as the incident angle modifier (K) are used in the optical efficiency definition:

$$\eta_{opt} = \rho \times \gamma \times \tau \times \alpha \times K(\theta)$$
$$\eta_{opt} = \rho \times \gamma \times \tau \times \alpha \times K(\theta) \quad (3)$$

The incident angle modifier for the examined collectors, LS-2, is given according to the following equation, as a function of the incident angle (θ) in degrees

$$K(\theta) = 1 - 2.2307 \times 10^{-4}\theta - 1.1 \times 10^{-4}\theta^2 + 3.18596 \times 10^{-6}\theta^3 - 4.85509 \times 10^{-8}\theta^4$$
$$K(\theta) = 1 - 2.2307 \times 10^{-4}\theta - 1.1 \times 10^{-4}\theta^2 + 3.18596 \times 10^{-6}\theta^3 - 4.85509 \times 10^{-8}\theta^4$$
(4)

The calculation of the final reflectance is a complex issue because many factors have to be taken into account,

except the reference reflectance (ρ_0). Equation 5 shows that the final reflectance (ρ) is a product of many factors with each one to represent a different optical loss

$$\rho = \rho_0 \cdot \rho_1 \cdot \rho_2 \cdot \rho_3 \cdot \rho_4 \cdot \rho_5 \cdot \rho_6$$
$$\rho = \rho_0 \cdot \rho_1 \cdot \rho_2 \cdot \rho_3 \cdot \rho_4 \cdot \rho_5 \cdot \rho_6 \quad (5)$$

The shadow effect is taken into account with (ρ_1), the twisting error with (ρ_2), the geometric errors with (ρ_3), the mirror clearness with (ρ_4), the receiver clearness with (ρ_5) and the other possible errors with (ρ_6). According to the literature, the receiver clearness can be estimated according to the next equation, using the mirror clearness

$$\rho_5 = \frac{1+\rho_4}{2}\rho_5 = \frac{1+\rho_4}{2} \quad (6)$$

The useful heat production (Q_u) can be alculated by the energy balance in the working fluid volume, as it is presented below:

$$Q_u = m.C_p.(T_{out} - T_{in})Q_u = m.C_p.(T_{out} - T_{in}) \quad (7)$$

The thermal efficiency (η_{th}) of the solar collector is equal to the ratio of the produced useful heat to the available solar energy (Qs). Equation 8 is the definition of the collector thermal efficiency:

$$\eta_{th} = \frac{Q_u}{Q_s}\eta_{th} = \frac{Q_u}{Q_s} \quad (8)$$

The useful heat can be also calculated by examining the heat transfer between the absorber tube and the working fluid temperature. The mechanism of the heat transfer is the convection which is modeled by using the heat transfer coefficient (h_{fluid}), as equation 9 indicates:

$$Q_u = h_{fluid} \times A_{r1} \times (T_r - T_{fluid})$$
$$Q_u = h_{fluid} \times A_{r1} \times (T_r - T_{fluid}) \quad (9)$$

The mean fluid temperature (T_{fluid}) can be calculated as the mean value of the inlet (Tin) and the outlet (T_{out}) fluid temperatures. This temperature level is also used for the working fluid properties calculation.

$$T_{fluid} = \frac{T_{in}+T_{out}}{2}T_{fluid} = \frac{T_{in}+T_{out}}{2} \quad (10)$$

The heat transfer coefficient can be estimated by using the Nusselt number which is defined as:

$$N_{u,fluid} = \frac{h_{fluid} \times D_{r1}}{k_{fluid}}N_{u,fluid} = \frac{h_{fluid} \times D_{r1}}{k_{fluid}} \quad (11)$$

For turbulent flow, as in the present study for all the examined cases (Re>2300), the Nusselt number can be calculated by using the Dittus-Boelter equation:

$$N_{u,fluid} = 0.023 \times Re_{fluid}^{0.8} \times Pr_{fluid}^{0.4}$$
$$N_{u,fluid} = 0.023 \times Re_{fluid}^{0.8} \times Pr_{fluid}^{0.4} \quad (12)$$

The Reynolds number (Re) and the Prandtl number (Pr) are defined as equations 13 and 14 indicate

$$Re_{fluid} = \frac{4.m}{\pi.D_{r1}.\mu_{fluid}}Re_{fluid} = \frac{4.m}{\pi.D_{r1}.\mu_{fluid}} \quad (13)$$

$$Pr_{fluid} = \frac{\mu_{fluid}.C_{p,fluid}}{k_{fluid}}Pr_{fluid} = \frac{\mu_{fluid}.C_{p,fluid}}{k_{fluid}} \quad (14)$$

The developed thermal model is based on the energy balance on the absorber tube. The absorbed solar energy (Qabs) is separated to useful heat (Qu) and to thermal losses (Q_{loss}), as it is shown below:

$$Q_{abs} = Q_u + Q_{loss}\,Q_{abs} = Q_u + Q_{loss} \quad (15)$$

The thermal losses of the solar collector can be calculated by examining the heat transfer mechanism from the absorber to the cover. Due to vacuum between absorber and cover (pressure level of some Pascal), the convection phenomenon is neglected, and only the radiation thermal losses have to be taken into consideration

$$Q_{loss} = \frac{A_{r0} \times \sigma \times (T_r^4 - T_c^4)}{\frac{1}{\epsilon_r} + \frac{1-\epsilon_c}{\epsilon_c}\left(\frac{A_{r0}}{A_{c1}}\right)}Q_{loss} = \frac{A_{r0} \times \sigma \times (T_r^4 - T_c^4)}{\frac{1}{\epsilon_r} + \frac{1-\epsilon_c}{\epsilon_c}\left(\frac{A_{r0}}{A_{c1}}\right)} \quad (16)$$

The receiver emittance is taken as a function of its temperature level. A literature equation for cermet coating is given below:

$$\epsilon_r = 0.05599 + 1.039 \times 10^{-4}.T_r + 2.249 \times 10^{-7}.T_r^2$$
$$\epsilon_r = 0.05599 + 1.039 \times 10^{-4}.T_r + 2.249 \times 10^{-7}.T_r^2 \quad (17)$$

In steady state conditions, as in the examined model, the thermal losses from the absorber to the cover are equal to the thermal losses from the cover to the ambient. These thermal losses include radiation and convection losses, as it is given below

$$Q_{loss} = h_{air} \times A_{c0} \times (T_c - T_{am}) + A_{c0}.\sigma.\in_c (T_c^4 - T_{sky}^4)$$
$$Q_{loss} = h_{air} \times A_{c0} \times (T_c - T_{am}) + A_{c0}.\sigma.\in_c (T_c^4 - T_{sky}^4)$$
(18)

It is important to state that the sky temperature (T_{sky}) has been used in the radiation losses term and this temperature level can be estimated by equation 19 for clear skies

$$T_{sky} = 0.0553 \times T_{am}^{1.5} T_{sky} = 0.0553 \times T_{am}^{1.5}$$
(19)

The heat convection coefficient between the cover and the ambient air is calculated by using a literature equation for the Nusselt number:

$$N_{u,air} = 0.193 \times Re_{air}^{0.618} \times Pr_{air}^{0.33}$$
$$N_{u,air} = 0.193 \times Re_{air}^{0.618} \times Pr_{air}^{0.33}$$
(20)

It is important to give the definition of the Nusselt and of the Reynolds number for this case. The outer diameter of the cover tube (D_{co}) is used as the characteristic length:

$$N_{u,air} = \frac{h_{air} \times D_{co}}{k_{air}} N_{u,air} = \frac{h_{air} \times D_{co}}{k_{air}}$$
(21)

$$Re_{air} = \frac{\mu_{air} \times D_{co}}{v_{air}} Re_{air} = \frac{\mu_{air} \times D_{co}}{v_{air}}$$
(22)

Moreover, it is useful to state that the air properties are calculated to the mean temperature between cover and ambient (Tc-am), as it is given below

$$T_{c-am} = \frac{T_c + T_{am}}{2} T_{c-am} = \frac{T_c + T_{am}}{2}$$
(23)

The pressure losses along the absorber tube (ΔP) can be calculated according to the following equation:

$$\Delta P = f_r \times \frac{L}{D_{ri}} \left(\frac{1}{2} \times \rho_{fluid} . u_{fluid}^2\right)$$
$$\Delta P = f_r \times \frac{L}{D_{ri}} \left(\frac{1}{2} \times \rho_{fluid} . u_{fluid}^2\right)$$
(24)

The friction factor (fr) is calculated according to equation 25, for turbulent flow

$$f_r = \frac{1}{[0.79.\ln(Re_{fluid}) - 1.64]^2} f_r = \frac{1}{[0.79.\ln(Re_{fluid}) - 1.64]^2}$$
(25)

The mean working fluid velocity is calculated as:

$$u_{fluid} = \frac{m}{\rho_{fluid} \cdot \left(\pi \times \frac{D_{ri}^2}{4}\right)} u_{fluid} = \frac{m}{\rho_{fluid} \cdot \left(\pi \times \frac{D_{ri}^2}{4}\right)}$$
(26)

Moreover, it is useful to give the definition of the volumetric flow of the working fluid:

$$V_{fluid} \left(\frac{l}{min}\right) = (60000) \times u_{fluid} \times \left(\pi \frac{D_{ri}^2}{4}\right)$$
$$V_{fluid} \left(\frac{l}{min}\right) = (60000) \times u_{fluid} \times \left(\pi \frac{D_{ri}^2}{4}\right)$$
(27)

The exergetic analysis of the solar collector is performed by making a detailed analysis which includes the exergy of the solar irradiation, the useful exergy production, the exergetic losses and the exergy destruction. Parabolic trough collectors utilize only the beam irradiation which can be assumed to be undiluted. Thus, the Petela model can be used for estimating the exergy flow on the incoming solar irradiation. This model takes into account that the sun is a radiation reservoir of temperature (Tsun), which is estimated to be 5770 K in the outer layers. Equation 28 shows the exergy flow of the undiluted solar irradiation (Es):

$$E_s = Q_s . \left[1 - \frac{4}{3} . \left(\frac{T_{am}}{T_{sum}}\right) + \frac{1}{3} \left(\frac{T_{am}}{T_{sum}}\right)^4\right]$$
$$E_s = Q_s . \left[1 - \frac{4}{3} . \left(\frac{T_{am}}{T_{sum}}\right) + \frac{1}{3} \left(\frac{T_{am}}{T_{sum}}\right)^4\right]$$
(28)

The useful exergy output can be calculated according to the following equation

$$E_u = Q_u - m . C_p . T_{am} . \ln\left[\frac{T_{out}}{T_{in}}\right] - m . T_{am} \frac{\Delta P}{\rho_{fluid} . T_{fm}}$$
$$E_u = Q_u - m . C_p . T_{am} . \ln\left[\frac{T_{out}}{T_{in}}\right] - m . T_{am} \frac{\Delta P}{\rho_{fluid} . T_{fm}}$$
(29)

Equation 29 can be applied to both liquid and gas working fluids. Especially for liquids, the last term of the pressure drop (ΔP) is usually small and can be neglected. On the other hand, the operation with gas working fluids is associated with high pressure losses, due to the low density of the gases, and it has to be taken into account.

The exergetic efficiency of the solar collector (η_{ex}) is defined as the ratio of the useful production to the exergy input, as the following equation indicate

$$\eta_{ex} = \frac{E_u}{E_s}\eta_{ex} = \frac{E_u}{E_s} \quad (30)$$

Finally, it is important to give the total exergy balance of the system:

$$E_s = E_u + E_{loss} + E_d E_s = E_u + E_{loss} + E_d \quad (31)$$

In the similar way, the energy and exergy analysis for waste heat recovery cycles such as supercritical carbon-di-oxide system, organic Rankine cycle (ORC), as well as remaining auxiliary components can be computed.

6. CONCLUSIONS

In this study thermodynamic analysis of PTSC integrated combined cycle (PSCO2–ORC) was presented. Following conclusions were made

- The combined cycle performance was enhanced with the solar irradiation. The PSCO2 cycle is 1–3% more efficient than that previously proposed without a partial heating cycle.
- PSCO2 cycle thermal efficiency increased by 4.47% after ORC integration.
- Maximum combined cycle (PSCO2–ORC) thermal and exergetic efficiency without taking into account the performance of PTSCs was achieved by 48.61 and 83.26%, respectively, while taking into account the performance of PTSCs, its exergy performance was reduced to 42.31%.
- Combined cycle output was also marginally improved with turbine inlet pressure and recuperator efficiency Pressure and effectiveness are turbine and recuperator design parameters, respectively.
- PTSCs alone account for 62.93% of total exergy destruction, which is around 8027 kW. This doesn't mean the worst system is PTSCs. It is based only on exergetic performance.
- Maximum total exergy destruction was found at 9259.12 kW and 12962.64 kW for combined cycle and overall plant, respectively.
- The combined cycle performance was decreased and improved with the angle of solar incidence and the split ratio, respectively. The lower the angle of incidence, the higher the performance of the PTSC. Therefore, a reduction in the incidence of solar beam is required for higher PTSC performance.
- Working fluid R1233zd(E) is recommended for power generation in the ORC bottoming system. In addition, R1243zf is found to be the worst working fluid among selected fluids in this study.
- The combined cycle's exergetic performance was reduced due to the performance of the PTSCs.
- Thermoeconomic and exergoeconomic analysis of the PTSC integrated combined (PSCO2– ORC) cycle may be carried out in future research. Practical applications for generating power in desert areas are also feasible where traditional heat sources are not available.

7. RESULTS

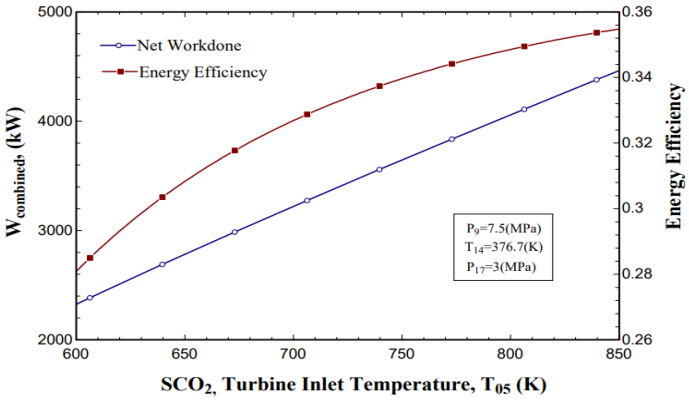

Figure 2 Effect of Turbine inlet temperature of topping cycle on combined work output and energy efficiency of the system.

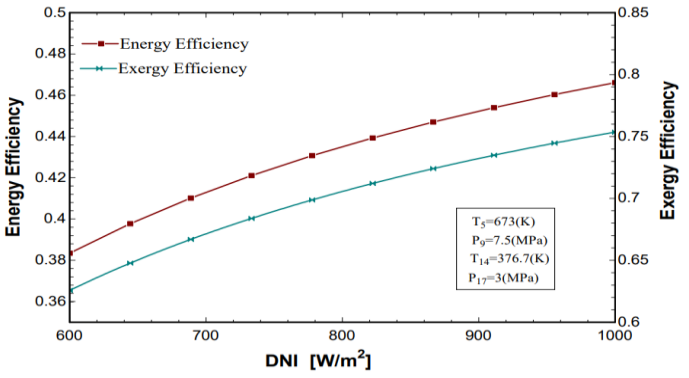

Figure 3 Effect of Direct normal Irradiance (DNI) on energy and exergy efficiency of the system.

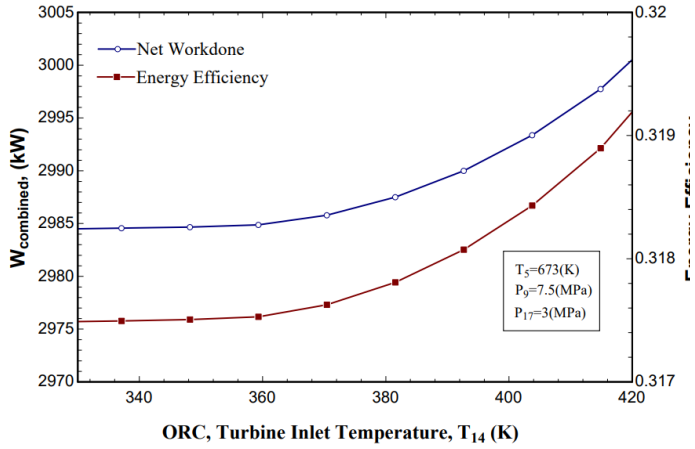

Figure 4 Effect of Turbine inlet temperature of bottoming cycle on combined work output and energy efficiency of the system.

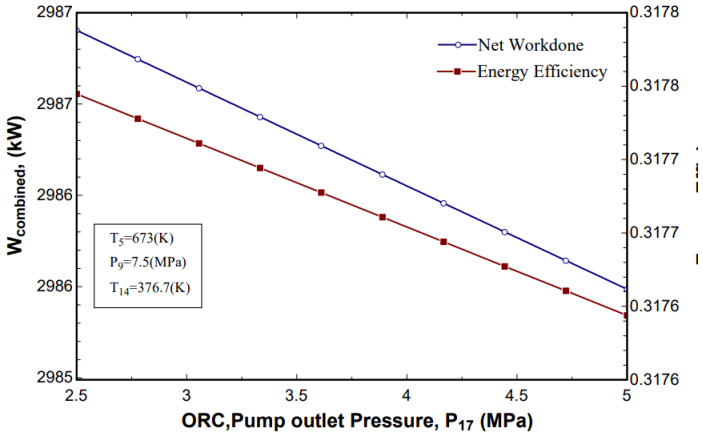

Figure 5 Effect of Pump outlet pressure of bottoming cycle on combined work output and energy efficiency of the system.

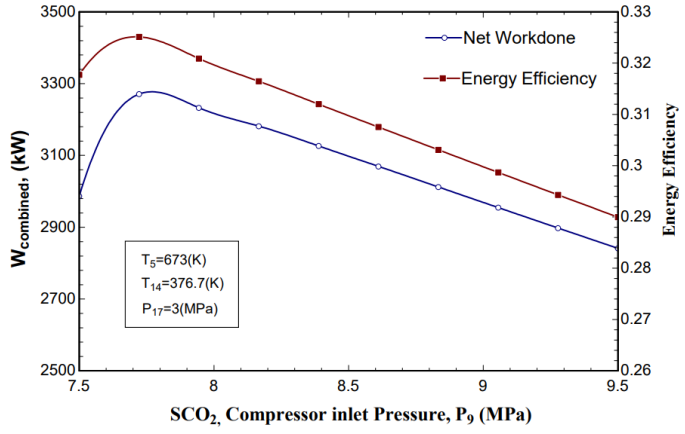

Figure 6 Effect of compressor inlet pressure on combined work output and energy efficiency of the system.

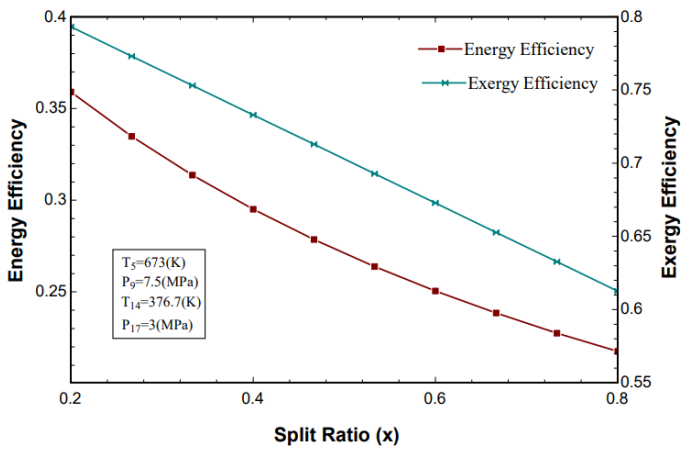

Figure 7 Effect of split ratio on energy and exergy efficiency of the system.

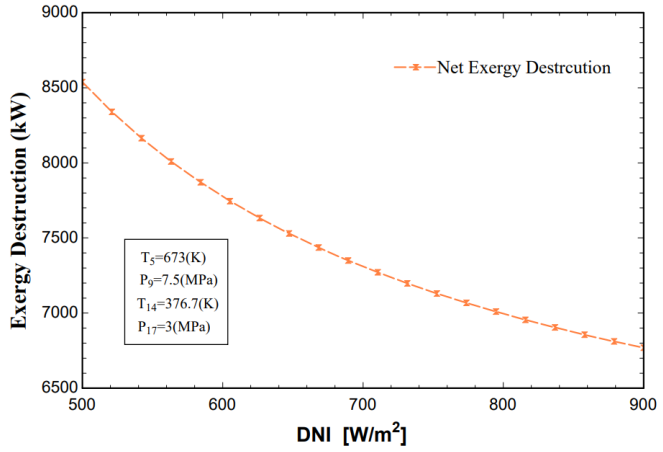

Figure 8 Effect of DNI on exergy destruction of the system.

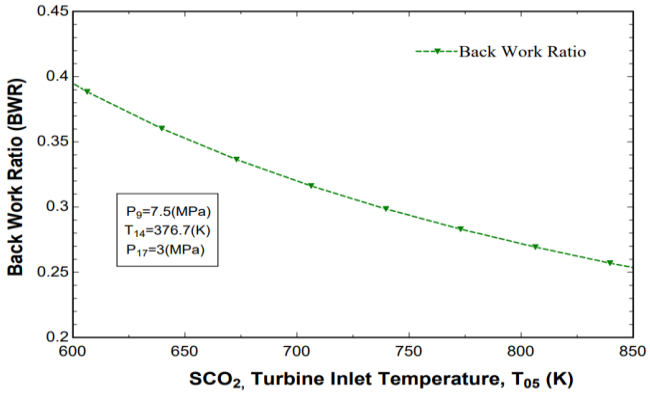

Figure 9 Effect of Turbine inlet temperature of topping cycle on back work ratio of the topping cycle.

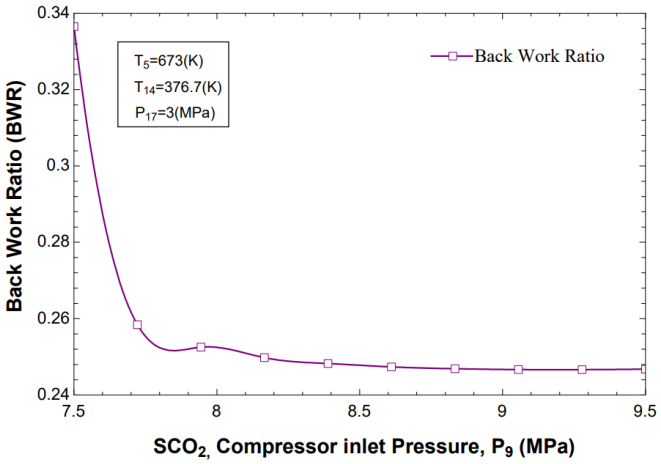

Figure 10 Effect of compressor inlet pressure on back work ratio of the topping cycle.

8. REFERENCES

1. Abam, F. I., T. A. Briggs, E. B. Ekwe, C. G. Kanu, S. O. Effiom, M. C. Ndukwu, S. O. Ohunakin, and M. I. Ofem. 2018. Exergy analysis of a novel low-heat recovery organic Rankine cycle (ORC) for combined cooling and power generation. Energy Sources, Part A: Recovery, Utilization, and Environmental Effects 41(13):164962.doi:10.1080/15567036.2018.1549140.

2. Abdelghani-Idrissi, M., S. Khalfallaoui, D. Seguin, L. Vernières-Hassimi, and S. Leveneur. 2018. Solar tracker for enhancement of the thermal efficiency of solar water heating system. Renewable Energy 119:79–94. doi:10.1016/j. renene.2017.11.072.

3. Ahn, Y., S. J. Bae, M. Kim, S. K. Cho, S. Baik, J. I. Lee, and J. E. Cha. 2015. Review of supercritical CO2 power cycle technology and current status of research and development. Nuclear Engineering Technology47(6):64761.doi:10.1016/j.net.2015.06.009.

4. Al-Sulaiman, F. A. 2013. Energy and sizing analyses of parabolic trough solar collector integrated with steam and binary vapor cycles. Energy 58:561–70. doi:10.1016/j.energy.2013.05.020.

5. Al-Sulaiman, F. A. 2014. Exergy analysis of parabolic trough solar collectors integrated with combined steam and organic Rankine cycles. Energy Conversion and Management 77:441–49. doi:10.1016/j.enconman.2013.10.013.

6. Al-Sulaiman, F. A., F. Hamdullahpur, and I. Dincer. 2012. Performance assessment of a novel system using parabolic trough solar collectors for combined cooling, heating, and power production. Renewable Energy48:16172.doi:10.1016/j.renene.2012.04.034.

7. Al-Zahrani, A. A., and I. Dincer. 2018. Energy and exergy analyses of a parabolic trough solar power plant using carbon dioxide power cycle. Energy Conversion and Management 158:476–88. doi:10.1016/j.enconman.2017.12.071.

8. Ashouri, M., A. M. K. Vandani, M. Mehrpooya, M. H. Ahmadi, and A. Abdollahpour. 2015. Techno-economic assessment of a Kalina cycle driven by a parabolic Trough solar collector. Energy Conversion and Management 105:1328–39. doi:10.1016/j.enconman.2015.09.015.

9. Bellos, E., and C. Tzivanidis. 2016. Parametric analysis and optimization of a solar driven trigeneration system based on ORC and absorption heat pump. Journal of Cleaner Production 161:493–509. doi:10.1016/j.jclepro.2017.05.159.

10. Ben, M. C., M. F. Aissa, S. Bouadila, M. Balghouthi, A. Farhat, and A. Guizani. 2016. Experimental investigation of parabolic trough collector system under Tunisian climate: Design, manufacturing and performance assessment. Applied Thermal Engineering101:27383.doi:10.1016/j.applthermaleng.2016.02.073.

11. Besarati, S. M., and D. Y. Goswami. 2014. Analysis of advanced supercritical carbon dioxide power cycles with a bottoming cycle for concentrating solar power applications. Journal of Solar Energy Engineering 136 (1):010904- 1-7. doi:10.1115/1.4025700.

12. Cabrera, F., A. Fernández-García, R. Silva, and M. Pérez-García. 2013. Use of parabolic trough solar collectors for solar refrigeration and air-conditioning applications. Renewable and Sustainable Energy Reviews 20:103–18. doi:10.1016/j. rser.2012.11.081.

13. Campanari, S., and E. Macchi.1998. Thermodynamic analysis of advanced power cycles based upon solid oxide fuel cells, gas turbines and Rankine bottoming cycles. 98-GT-585, ASME International Gas Turbine and Aeroengine Congress and Exhibition, Stockholm, Sweden. June, 2e5. Cengel, Y. A., and M. A. Boles.

2004. Thermodynamics an engineering approach. 5th ed. McGraw-Hill publication. ENERGY SOURCES, PART A: RECOVERY, UTILIZATION, AND ENVIRONMENTAL EFFECTS 25 Delgado-Torres, A. M., and L. García-Rodríguez. 2010a. Preliminary design of seawater and brackish water reverse osmosis desalination systems driven by low temperature solar organic Rankine cycles (ORC). Energy Conversion and Management 51 (12):2913–20. doi:10.1016/j.enconman.2010.06.032.

14. Delgado-Torres, A. M., and L. García-Rodríguez. 2010b. Analysis and optimization of the low-temperature solar organic Rankine cycle (ORC). Energy Conversion and Management 51 (12):2846–56. doi:10.1016/j.enconman.2010.06.022.

15. Delgado-Torres, A. M., L. García-Rodríguez, and V. J. Romero-Ternero. 2007. Preliminary design of a solar thermal-powered seawater reverse osmosis system. Desalination 216 (1–3):292–305. doi:10.1016/j. desal.2006.12.015.

16. Singh, H., and R. S. Mishra. 2018b. Energy- and exergy-based performance evaluation of solar powered combined cycle (recompression supercritical carbon dioxide cycle/organic Rankine cycle). Clean Energy 1–14. Song, J., X.-S. Li, X.-D. Ren, and C.-W. Gu. 2018. Performance analysis and parametric optimization of supercritical carbon dioxide (S-CO2) cycle with bottoming Organic Rankine Cycle (ORC). Energy 143:406–16. doi:10.1016/j. energy.2017.10.136.

NOMENCLATURE

A co	Absorber cover's area m2
D	diameter (m)
Q_	Heat transfer (kW)
C p	Specific heat (kJ/kg-K)
Cols	Number of collectors in a row
Col p Dco; o ORC	Number collectors in parallel rows Cover's outside diameter, m organic Rankine cycle
Ex	exergy,(kW)
m_ HTF :	HTF mass flow rate, kg/s
Ed	Exergy destruction rate
Comp	compressor
Cond	condenser
Nu h HX	Nusselt number specific enthalpy heat exchanger
SCO2 kair V s PSCO2	super critical CO2 Thermal conductivity of air volume flow rate (m3/s) specific entropy,(kJ/kg-K) partial heating super critical CO2 cycle
T	temperature (K)
T0	atmospheric temperatures
W	Collector's width
W_SCO2,T ORC,T	Work per unit time SCO2 turbine ORC turbine

BIOGRAPHIES

Prof, Ajay Kashikar is working as a assistant professor in department of mechanical engineering at lokmanya tilak college of engineering, Navi Mumbai. His research interest includes Thermodynamic analysis, solar, electric vehicles, Computational fluid dynamic analysis. etc.

.

Reshma Bangar is a student pursuing her masters from Alamuri Ratnamala institute of engineering and technology, Shahpur, Thane. Her research interest includes thermodynamics, heat transfer analysis, power plant, solar, SOFC etc.